Density Functional Theory Study of the Adsorption of Thiophene on NiMoS Surface

Wahyu A E Prabowo, M Kemal Agusta, Nugraha, Subagjo, Ahmad H Lubis, Hermawan K Dipojono

***Abstract*—In the last decades, research on hydrotreating has regularly been intensified due mainly to reaching cleaner environmentally based international fuel standards. Among the processes used to refine petroleum cuts, hydrodesulfurization (HDS) is a key process to reduce sulfur contents in diesel and gasoline below 10 ppm. Transition metal sulfide catalysts such as MoS_2 phase promoted by Ni(MoS) are known to be selective for the hydrodesulfurization reaction. The experimentally observed higher selectivity of NiMoS is explained on the basis of the reactants adsorption selectivity and the evaluation of the active edge energies with the adsorbed reactants. To uncover the physical phenomena responsible for the adsorption of thiophene on the NiMoS active edge sites, the electronic structure of the recommended material is investigated by using density functional theory (DFT). The adsorption energy of thiophene in the top site of Ni atom is - 12.94 kcal/mol or it is about -0.56 eV, while in the top site of Mo atom is -36.88 kcal/mol or it is about -1.5 eV. These findings are consistent with other theoretical calculations. We believe that it is responsible for the hydrodesulfurization reaction (HDS) and it will give additional insights of reducing sulfur contents.**

***Index Terms*—NiMoS, thiophene (C_4H_4S), hydrodesulfurization (HDS), density functional theory.**

I. Introduction

THE refinement of crude oil is one of the cornerstones of modern society. In this chemical process, the crude oil is converted into transportation fuels, such as gasoline and diesel oil. An important step in oil refining is the catalytic hydrotreating of liquid petroleum fractions, which are obtained after distillation of the crude oil. During catalytic hydrotreating, the hetero-atoms N, S, and O are removed from the petroleum fractions. SO_2 and NO_x are formed during the combustion of the hydrocarbon contains those hetero-atoms. These new products, SO_2 and NO_x are main contributors to the formation of acid rain. Furthermore, these types of hydrocarbon have a detrimental effect on the transition-metal based catalysts used in further refining processes and in car exhausts. Hydrotreating converts olefins and aromatics into saturated hydrocarbon, which burn more cleanly (i.e. fully to CO_2 and H_2O). The annual sale of hydrotreating catalysts is 30% of the total global catalyst market, which emphasizes the importance of hydrotreating. In particular, the hydrodesulfurization (HDS) is a key process to reduce sulfur contents in diesel and gasoline below 10 ppm. These environmental constraints represent a driving force for the continuous improvement of the γ alumina NiMoS supported catalysts that is widely used in the refining industry [1], [2].

The HDS of gasoline produced from the fluid catalytic cracking (FCC) unit requires a selective sulfur removal from thiophene derivatives while avoiding the hydrogenation of olefins (HydO) present in FCC gasoline. This represents a technical challenge to prevent the loss of octane number of gasoline. The HDS selectivity has been the subject of recent experimental works on model molecules for FCC gasoline or real feed [3], [4], [5], [6], [7], [8]. Numerous experimentals [9], [10], [11], [12], [13], [14], [15], [16], and theoretical works [17], [18], [19], [20], [21], [22], [23], have provided atomistic descriptions of the NiMoS active phases. Although some experimental investigations on NiMoS active phase had been conducted in the recent years, however some problems remain unresolved. A starting point to begin with is uncovering the adsorption of thiophene on NiMoS surface. The density functional theory (DFT) [24], [25] based on ab initio computational method will be used for this purpose.

II. Computational Details

The calculations are implemented in the opEn Source Package for Research in Electronic Structure, Simulation, and Optimization (Quantum ESPRESSO) [26]. The ultrasoft pseudopotential method is employed to describe the interaction between ion cores and electrons. The electron exchange correlation is treated by a generalized gradient approximation (GGA) based on Perdew, Burke, and Ernzerhof (PBE) functional [27]. The planewave basis set with a cutoff energy of 340 eV is used for all calculations.

We use a supercell (12.294 x 10.683 x 20.120) $\mathring{A}$ for NiMoS model with 48 atoms, namely 32 atoms (S), 12 atoms

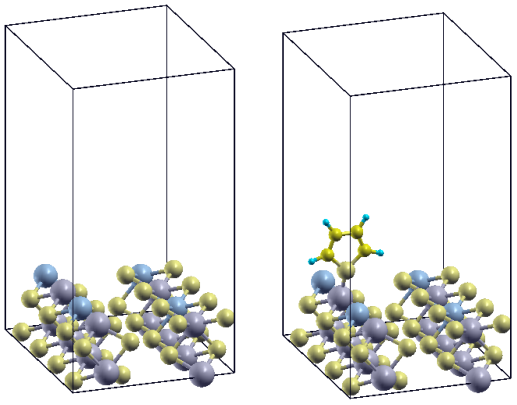

Fig. 1. On the left, showing the NiMoS surface. On the right, showing the thiophene adsorbed in NiMoS surface. (gold: S atom, grey: Mo atom, blue: Ni atom, yellow: C atom, green: H atom)

Manuscript received January 08, 2013; revised January 23, 2013. This work was supported by partial financial from Directorate General of Higher Education of Republic of Indonesia through the Decentralization of Research Grant Project.

Wahyu, Kemal, Nugraha and Hermawan are with the Department of Engineering Physics, and Subagjo is with the Department of Chemical Engineering, Bandung Institute of Technology, Bandung, 40132 Indonesia e-mail: wahyu.a.e.prabowo@gmail.com

Ahmad is with the Department of Electrical Engineering, Al Azhar Indonesia University, Jakarta, 12110, Indonesia

ISBN: 978-988-19252-6-8
ISSN: 2078-0958 (Print); ISSN: 2078-0966 (Online)

(Mo), and 4 atoms (Ni), respectively. The Monkhorst-Pack method [28] is used to sample k-points by using 3x3x1 grid. Based on the model, the four Mo edge atoms in the surface are substituted by Ni promoter atoms in the NiMoS surface.

Figure 1 shows the structure of the NiMoS surface with the vacuum layer of 16.6 $\mathring{A}$, which is located above NiMoS surface in the z direction to avoid interactions between surfaces. Figure 2 shows the initial condition for thiophene before being adsorbed in NiMoS surface.

III. Results and Discussion

A. Optimization Geometry

1) Optimization Geometry of Thiophene: Thiophene is a group of substrates especially common in petroleum. The thiophene content is removed through HDS process. Many kinds of thiophene derivative are formed in petroleum ranging from thiophene itself to more complicated ones like benzothiophenes and dibenzothiophenes. Thiophene itself and its alkyl derivatives are easier to be hydrogenalized. Whereas dibenzothiophene particularly its 4,6-disubstituted derivatives are considered to be the most challenging substrates. Benzothiophenes are midway between the thiophenes and dibenzothiophenes in their susceptibility to HDS. Therefore, we start with thiophene to investigate HDS.

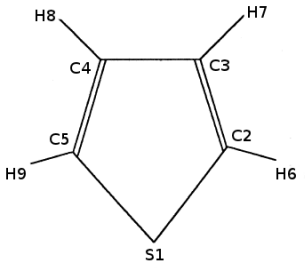

Fig. 2. Thiophene (C_4H_4S) molecular model and atom numbering scheme.

TABLE I
Geometric parameters for the Optimized isolated thiophene

Distance ($\mathring{A}$)	Experimental	Calculated[a]	Calculated[b]
S_1-C_2	1.71	1.73	1.71
S_1-C_5	1.71	1.73	1.71
C_2-C_3	1.37	1.37	1.37
C_3-C_4	1.42	1.43	1.42
C_4-C_5	1.37	1.37	1.37

The final thiophene optimized-structure is displayed in Table I. From the computational results, one may conclude that the values of the optimization geometry depend on the calculational method of the same scheme of calculation. If we compare the final result of the optimized structure of thiophene with the experimental and other computational calculation[a] by Itamar *et al* [29], they will be in a good agreement. Itamar *et al* calculations were done using the B3LYP functional. They used the G03 default parameters and quadratic convergence (QC) methods to improve DFT calculation. In our calculations[b], we used Perdew, Burke, and Ernzerhof (PBE) functional for exchange correlation energy.

In our calculations[b], the distance of (S_1-C_2 is 1.70 $\mathring{A}$), (C_2-C_3 is 1.37 $\mathring{A}$), (C_3-C_4 is 1.42 $\mathring{A}$) have a good agreement with the experimental result.

Table II shows the comparation of the angle in thiophene structure. Our result[b] is in a good agreement with that of Kochikov *et al*[a] [30].

TABLE II
Structure comparation for the isolated thiophene

Angle (^{0})	Calculated[a]	Calculated[b]
$\angle$ C_2-S_1-C_5	92.4	92.3
$\angle$ S_1-C_2-C_3	111.6	111.3
$\angle$ C_2-C_3-C_4	112.2	112.4
$\angle$ S_1-C_2-H_6	119.9	120.1
$\angle$ C_4-C_3-H_8	124.4	124.3
$\angle$ C_3-C_2-H_6	128.5	128.4
$\angle$ C_2-C_3-H_7	123.4	123.1

2) Optimization Geometry of NiMoS and thiophene: The final NiMoS optimized structure is displayed in Figure 3. It is slightly different from the model obtained by Itamar *et al*. The model in this investigation consists two-side slabs where the upmost layer of each slabs contains two Ni atoms and two Mo atoms. Itamar *et al* used slightly different model with only one side slab and four Ni atoms in the uppermost layer. Using DFT with periodic boundary conditions, calculation for optimization of geometry is relevant with Itamar *et al* and from the experimental data and calculation from Raybaud *et al* [31]. Periodic boundary condition approach indicates that there is only a slightly distortion in local structure around the Ni atoms, not in the all of surface area. In spite of the distortion, distances between metal atoms are in good agreement with theoretical approach [29], [31].

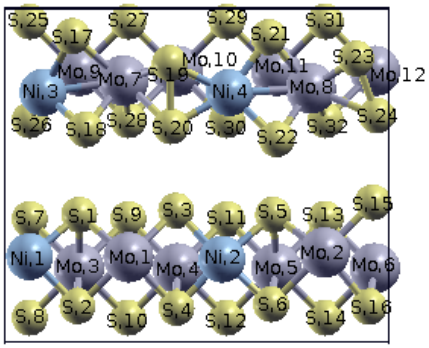

Fig. 3. Scheme of atomic number in z direction of NiMoS surface.

The Ni-Mo distances from extended X-ray adsorption fine structure experimental calculation and our DFT based calculation are in a good agreement with experimental data [15]. The distances of Ni_1-Mo_3, Ni_2-Mo_5, Ni_2-Mo_4, Ni_2-Mo_6, Ni_1-S_1, Ni_2-S_3, Ni_2-S_4 are also in a good agreement with experimental results [15]. The Ni-S distances are a bit larger than experimental values, and a slight distortion is also present. Overall, our calculation for NiMoS is relevant with Raybaud *et al*. The comparative studies of structure optimization are shown in Table III, containing four references:

ISBN: 978-988-19252-6-8
ISSN: 2078-0958 (Print); ISSN: 2078-0966 (Online)

[a]from Itamar *et al* [29], [b]work by us, *Exp* from Bouwens *et al* [15], and [c]from Raybaud *et al* [31].

TABLE III
STRUCTURE COMPARATION FOR NIMOS + THIOPHENE

Distance (Å)	Calculated[a]	Calculated[b]	Exp	Calculated[c]
Ni_1-Mo_3	2.66	2.96	2.85	2.75
Ni_2-Mo_5	2.86	2.96	2.85	2.75
Ni_2-Mo_4	2.76	2.79	2.85	2.75
Ni_2-Mo_6	5.46	5.45	-	-
Ni_1-S_1	2.30	2.19	-	2.17
Ni_2-S_3	2.25	2.19	-	2.17
Ni_2-S_4	2.25	2.14	-	2.17

Table IV shows the optimization of our calculation for NiMoS structure. There are two-side slabs in y direction. Both of them have appropriate distances.

TABLE IV
OPTIMIZED STRUCTURE FOR NIMOS SURFACE

Distance (Å)	Calculated	Distance	Calculated
Ni_1 - Mo_1	3.18	Ni_2 - Mo_2	3.31
Ni_1 - S_2	2.21	Ni_1 - Ni_2	6.16
Ni_1 - S_1	2.19	Mo_1 - Mo_2	6.28
Mo_1 - S_2	2.32	Ni_1 - Mo_3	2.96
Mo_1 - S_1	2.32	Mo_1 - Mo_3	3.23
Mo_1 - S_4	2.30	Mo_1 - Mo_4	3.22
Mo_1 - S_3	2.30	Ni_2 - Mo_4	2.79
Ni_2 - S_4	2.14	Ni_2 - Mo_5	2.96
Ni_2 - S_3	2.19	Mo_2 - Mo_5	3.20
Ni_2 - S_6	2.13	Mo_2 - Mo_6	3.23
Ni_2 - S_5	2.27	Ni_2 - Mo_3	5.17
Mo_2 - S_6	2.43	Ni_2 - Mo_6	5.45
Mo_2 - S_5	2.29	Ni_1 - Mo_4	5.36
Mo_2 - S_{15}	2.33	Mo_1 - Mo_5	5.50
Mo_2 - S_{16}	2.23	Mo_2 - Mo_4	5.48
Mo_1 - Ni_2	3.02	-	-
Ni_3 - Mo_7	2.60	Mo_8 - S_{23}	2.42
Mo_7 - Ni_4	3.60	Ni_3 - Mo_9	3.22
Ni_4 - Mo_8	2.73	Mo_7 - Mo_9	3.21
Ni_3 - S_8	2.11	Mo_7 - Mo_{10}	3.37
Ni_3 - S_7	2.30	Mo_7 - Mo_8	6.02
Mo_7 - S_8	2.28	Ni_3 - Ni_4	6.07
Mo_7 - S_{17}	2.44	Ni_2 - Mo_{10}	4.39
Mo_7 - S_{20}	2.55	Ni_4 - Mo_{11}	4.33
Mo_7 - S_{19}	2.48	Mo_8 - Mo_{12}	3.84
Ni_4 - S_{20}	2.18	Ni_3 - Mo_{10}	5.25
Ni_4 - S_{19}	2.26	Mo_7 - Mo_{10}	5.68
Ni_4 - S_{22}	2.14	Ni_4 - Mo_9	6.31
Ni_4 - S_{21}	2.18	Ni_4 - Mo_{12}	6.18
Mo_8 - S_{22}	2.23	Mo_8 - Mo_{10}	5.37
Mo_8 - S_{21}	2.34	Mo_8 - Mo_{11}	3.44
Mo_8 - S_{24}	2.48	-	-

B. Adsorption Energies of Thiophene

Adsorption of thiophene is a substantial starting step of the hydrodesulfurization process. It is impossible to activate the thiophene molecule suitable for further reaction, if the interaction of thiophene with a catalyst is too weak [32].

Adsorption energies are computed by optimized gas-phase thiophene, optimized NiMoS surface and optimized NiMoS/thiophene according to:

$$E_{ads} = E_{NiMoS/Thiophene} - (E_{NiMoS} + E_{Thiophene}) \quad (1)$$

where E_{ads} is adsorption energy, $E_{NiMoS/Thiophene}$ is total energy of NiMoS/thiophene system, E_{NiMoS} is total energy of NiMoS surface, and $E_{Thiophene}$ is total energy of thiophene.

This paper will focus on investigating the adsorption of thiophene in sites near Mo atom and Ni atom. The adsorption energy of thiophene in the top site of Ni atom is -12.94 kcal/mol or it is about -0.56 eV. Using similar orientation of the adsorbed thiophene, this result is in agreement with a periodic DFT calculation [32], that is -11.5 kcal/mol or it is about -0.49 eV. The DFT calculations [32] used a $Ni_1Mo_{15}S_{32}$ cluster with two Mo atoms on the corners and one Ni atom. Thiophene used only vertically adsorbed on top Ni atom in the metallic edge, with the adsorption energy at about -7.8 kcal/mol or -0.34 eV. Therefore, similar to the case of thiophene adsorption on bare MoS_2, the most favorable modes for a fully promoted metal edge are parallel to the metallic edge [32], [33], [34]. The distance of S atom in thiophene and Ni atom on the surface is 2.48 Å. So it is in good agreement with calculation by Orita *et al*, that is 2.26 Å. The adsorption structure of Ni atom on NiMoS surface is shown in Figure 4.

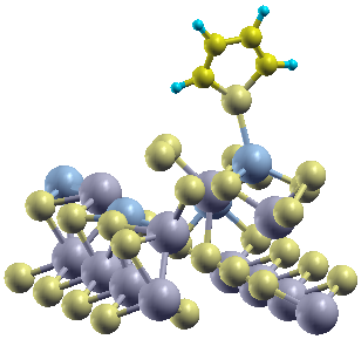

Fig. 4. Adsorption of thiophene in top site of Ni atom on NiMoS surface.

For the adsorption energy of thiophene in the top site of Mo atom is -36.88 kcal/mol or it is about -1.5 eV. This result is a bit larger than that of Orita *et al*, that is -25.37 kcal/mol or it is about -1.1 eV. This is due to the distortion of Mo atom with four S atom (Mo_3 with S_1, S_2, S_3, S_4), causing Mo atom bounded. The distance of S atom from thiophene and Ni atom from surface is 2.51 Å, a bit larger than that calculated by Orita *et al*, that is 2.35 Å. The adsorption structure of Mo atom on NiMoS surface is shown in Figure 5.

The experimental results of Hydrodesulfurization of transition metal sulfides is in a good agreement with a single volcano curve when it is plotted against the calculated bulk sulfur-metal bond strength [10]. In this case the variation in sulfur-metal bond strength is 1-2 eV and it is close to the adsorption energy of thiophene. This relationship is

ISBN: 978-988-19252-6-8
ISSN: 2078-0958 (Print); ISSN: 2078-0966 (Online)

explained by the basic idea that a value of sulfur-metal bond energy. Optimizes the appropriate interaction between sulfur organic compounds and CUS active sites [11].

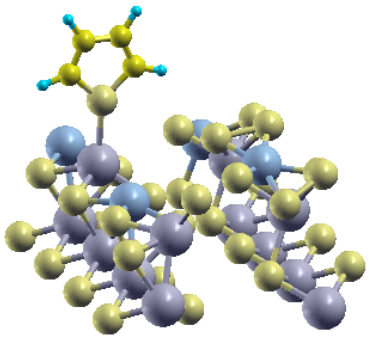

Fig. 5. Adsorption of thiophene in top site of Mo atom on NiMoS surface.

The next case we want to deal with is the interaction of NiMoS and thiophene in horizontal configuration. Here our calculation of energy yields -39.34 kcal/mol or at about -1.7 eV. This result is a bit different with that of Sun *et al* [35]. Their calculation shows that the energy adsorption for the thiophene with horizontal configuration is -48.2 kcal/mol or it is about -2.09 eV. Our system consists of two-side slabs (Figure 6), whereas that of Sun *et al* [35] used one cluster for their calculations. This is opening up many possibilities to get an adsorption energy from horizontal configuration. Although the above results are different, it is still consistent to the sulfur-metal bond strength energy of 1-2 eV and is almost identical to that in adsorption energy of thiophene.

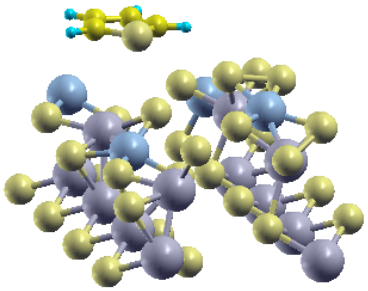

Fig. 6. Adsorption of thiophene with horizontal configuration on NiMoS surface.

IV. Conclusion

The adsorption of thiophene on NiMoS surface is investigated using DFT. Based on the model, by which four Mo edge atoms in the surface are substituted by Ni promoter atoms in the MoS_2 model. Geometry optimization of NiMoS surface, thiophene, and NiMoS/thiophene are carried out. Though the substitution of the Mo atom with Ni atom changes the structural and electronic properties of surface, but it is still a starting step to find a clear relation between HDS activity and electronic properties. The adsorption of thiophene on a surface has been studied by using vertical configuration on a replaced atom and followed by horizontal configuration. The variation in sulfur-metal bond strength is 1-2 eV and almost identical to that in adsorption energy of thiophene.

Acknowledgment

The authors would like to express their gratitude to the Office of ITB's Vice Rector for Research and Innovation for generous financial support to this investigation. Hermawan K Dipojono would like also to acknowledge the partial financial support from Directorate General of Higher Education of Republic of Indonesia through the Decentralization of Research Grant Project.

References

[1] R. Prins, in: G. Ertl, H. Knzinger, J. Weitkamp (Eds.), *Handbook of Heterogeneous Catalysis, vol. 4*, Wiley-VHC Verlagsgesellschaft, Weinheim, 1997, p. 1908.
[2] H. Topse, B.S. Clausen, F.E. Massoth, in: J.R. Anderson, M. Boudart (Eds.), *Hydrotreating Catalysis-Science and Technology*, Springer-Verlag, Berlin/Heidelberg, 1996, vol. 11.
[3] A. Daudin, S. Brunet, G. Perot, P. Raybaud, C. Bouchy, *J. Catal.* 248 (2007) 111.
[4] A.F. Lamic, A. Daudin, S. Brunet, C. Legens, C. Bouchy, E. Devers, *Appl. Cat. A* 344 (2008) 198.
[5] D. Mey, S. Brunet, C. Canaff, F. Maug, C. Bouchy, F. Diehl, *J. Catal.* 227 (2004) 436.
[6] S. Brunet, D. Mey, G. Perot, C. Bouchy, F. Diehl, *Appl. Catal. A* 278 (2005) 143.
[7] J.T. Miller, W.J. Reagan, J.A. Kaduk, C.L. Marshall, A.J. Kropf, *J. Catal.* 193 (2000)123-131.
[8] J.S. Choi, F. Mauge, C. Pichon, J. Olivier-Fourcade, J.C.Jumas, C. Petit-Clair, D.Uzio, *Appl. Catal. A* 267 (2004) 203.
[9] A. Daudin, A.F. Lamic, G. Perot, S. Brunet, P. Raybaud, C. Bouchy, *Catal. Today* 130 (2008) 221.
[10] H. Toulhoat, P. Raybaud, S. Kasztelan, G. Kresse, J. Hafner, *Catal. Today* 50 (1999) 629.
[11] R.R. Chianelli, G. Berhault, P. Raybaud, S. Kasztelan, J. Hafner, H. Toulhoat, *Appl. Catal. A* 227 (2002) 83.
[12] H. Toulhoat, P. Raybaud, *J. Catal.* 216 (2003) 63.
[13] J.V. Lauritsen, M.V. Bollinger, E. Lgsgaard, K.W. Jacobsen, J.K. Nrskov, B.S.Clausen, H. Topse, F. Besenbacher, *J. Catal.* 221 (2004) 510.
[14] J.V. Lauritsen, J. Kibsgaard, G.H. Olesen, P.G. Moses, B. Hinnemann, S. Helveg,J.K. Nrskov, B.S. Clausen, H. Topse, E. Laegsgaard, F. Besenbacher, *J. Catal.* 249 (2007) 220.
[15] S.M.A.M. Bouwens, J.A.R. van Veen, D.C. Koningsberger, V.H.J. de Beer, R. Prins, *J. Phys. Chem.* 95 (1991) 123.
[16] S. Kasztelan, H. Toulhoat, J. Grimblot, J.P. Bonnelle, *Appl. Catal.* 13 (1984) 127.
[17] H. Schweiger, P. Raybaud, H. Toulhoat, *J. Catal.* 212 (2002) 33.
[18] E. Krebs, B. Silvi, P. Raybaud, *Catal. Today* 130 (2008) 160.
[19] H. Schweiger, P. Raybaud, G. Kresse, H. Toulhoat, *J. Catal.* 207 (2002) 76.
[20] P. Raybaud, *Appl. Catal. A* 322 (2007) 76.
[21] L.S. Byskov, J.K. Nrskov, B.S. Clausen, H. Topse, *J. Catal.* 187 (1999) 109.
[22] A. Travert, H. Nakamura, R.A. van Santen, S. Cristol, J.F. Paul, E. Payen, *J. Am.Chem.Soc.* 124 (2002) 7084.
[23] M. Sun, A.E. Nelson, J. Adjaye, *J. Catal.* 226 (2004) 32.
[24] P. Hohenberg and W. Kohn, *Phys. Rev*, 136, B 864, 1964.
[25] W. Kohn and L.J.Sham, *Phys. Rev*, 140, A1133, 1965.
[26] Paolo G. et al, *Journal of Physics: Condensed Matter*, 21, 39, 2009.
[27] J. P. Perdew, K. Burke, M.Ernzerhof, *Phys. Rev. Lett*, 77, 3865, 1996.
[28] Monkhorst, H. J.; Pack, J. D. Phys. Rev. B 13 (1976) 5188.
[29] Itamar Borges Jr., and Alexander M. Silva, *J. Braz. Chem. Soc.*, 2012.
[30] Kochikov et al. *Journal of Molecular Structure* 567-568 (2001) 29-40
[31] Raybaud, P.; Hafner, J.; Kresse, G.; Kasztelan, S.; Toulhoat, H.; *J. Catal.* 2000, 190, 128.
[32] Hideo Orita, Kunio Uchida, Naotsugu Itoh, *Applied Catalysis A: General* 258 (2004) 115-120
[33] Cristol, S.; Paul, J. F.; Schovsbo, C.; Veilly, E.; Payen, E.; *J. Catal.* 2006, 239, 145.
[34] Silva, A. M.; Borges, I.; *J. Comput. Chem.* 2011, 32, 2186.
[35] Mingyong Sun, Alan E. Nelson, and John Adjayeb, *Catalysis Letters* Vol. 109, Nos. 3-4, July 2006